Synaptic transmission block by presynaptic injection of oligomeric amyloid beta

Herman Moreno[a,b], Eunah Yu[b,c], Gustavo Pigino[b,d], Alejandro I. Hernandez[e], Natalia Kim[e], Jorge E. Moreira[b,f], Mutsuyuki Sugimori[b,c], and Rodolfo R. Llinás[b,c,1]

Departments of [a]Neurology and Physiology/Pharmacology, and [e]Pathology, The Robert F. Furchgott Center for Neural and Behavioral Science, State University of New York Downstate Medical Center, Brooklyn, NY 11203; [b]Marine Biological Laboratory, Woods Hole, MA 02543; [c]Department of Physiology and Neuroscience, New York University School of Medicine, New York, NY 10016; [d]Department of Anatomy and Cell Biology, University of Illinois, Chicago, IL 60612; and [f]Department of Cell and Molecular Biology, Riberão Preto School of Medicine, University of São Paulo, Ribeirão Preto, 14049-900, São Paulo, Brazil

Early Alzheimer's disease (AD) pathophysiology is characterized by synaptic changes induced by degradation products of amyloid precursor protein (APP). The exact mechanisms of such modulation are unknown. Here, we report that nanomolar concentrations of intraaxonal oligomeric (o)Aβ42, but not oAβ40 or extracellular oAβ42, acutely inhibited synaptic transmission at the squid giant synapse. Further characterization of this phenotype demonstrated that presynaptic calcium currents were unaffected. However, electron microscopy experiments revealed diminished docked synaptic vesicles in oAβ42-microinjected terminals, without affecting clathrin-coated vesicles. The molecular events of this modulation involved casein kinase 2 and the synaptic vesicle rapid endocytosis pathway. These findings open the possibility of a new therapeutic target aimed at ameliorating synaptic dysfunction in AD.

Alzheimer's disease | fluorescence microscopy | presynaptic voltage clamp | squid giant synapse | ultrastructure

Clinically, Alzheimer's disease (AD) is manifested as a progressive deterioration of selective populations of neurons affecting particular cognitive domains, with initial symptoms indicating a decline in memory function. From a neuropathology perspective, AD has 2 major characteristics: (*i*) accumulations of extracellular aggregated peptide known as beta amyloid (Aβ), which form the well-characterized senile plaques; and (*ii*) intracellular accumulation of an abnormally phosphorylated protein, tau, leading to the formation of neurofibrillary tangles. The early-onset familial form of AD (FAD) has a strong genetic association with the 42-aa species of the Aβ peptide (1–3). Also, autosomal dominant mutations in the genes for amyloid-β precursor protein (APP), presenilin 1 (PS1), and PS2 increase production of Aβ42 and correlate significantly with the FAD syndrome. Aβ is a cleavage product of APP via the sequential action of 2 protease activities, the β secretase and the γ secretase complex (4, 5); β secretase cleaves APP at the N terminus, producing the membrane-bound moiety C99 and the secreted APPsβ segment. Subsequently, C99 is cleaved by the γ secretase to generate the C terminus of Aβ, resulting in a series Aβ peptides that are 38 to 43 aa in length. Under normal conditions, such events result in a higher proportion of Aβ40 over Aβ42 moieties. Under pathological conditions, such as in transgenic mice harboring human APP mutations, the production of Aβ42 increases, followed by many pathophysiological features of AD, including amyloid plaques, dystrophic neurites, and synaptic dysfunction (5). Despite strong evidence that Aβ42 is responsible for age-related memory decline, in humans, the extent of Aβ accumulation correlates poorly with memory abnormalities (6). Indeed, a specific challenge in addressing Aβ in AD concerned the role of specific aggregated pools of Aβ (e.g., extracellular, intracellular, membrane-associated, or insoluble) in the genesis of the pathology. Recently, AD symptoms were determined to be significantly correlated with intracellular and membrane-bound Aβ42 pools (7). However, intracellular Aβ42 was found to move

centrifugally from its origin at the somata (8). However, the differential dendritic and/or axonal distribution of this dispersive wave is still undetermined.

Thus, although there is evidence for synaptic dysfunction induced by oligomeric (o)Aβ, the pre or postsynaptic sites of action and the specific mechanisms responsible for such dysfunction have not been established. To help address these issues, we studied the consequences of acute intracellular versus extracellular oAβ42 exposure on synaptic transmission. The experimental design addressed: (*i*) possible functional and structural changes produced by intraaxonal Aβ peptides; and (*ii*) the molecular targets of Aβ peptides at the synapse.

The results obtained indicate that acute exposure to oAβ42 peptides disrupts synaptic transmission by altering the activity of a specific serine/threonine kinase, casein kinase 2 (CK2), which results in a reduction of synaptic vesicle pools on synaptic stimulation. This effect occurs only when the oAβ42 peptides are present in the presynaptic compartment. The effect of oAβ42 was compared with that of oAβ40, which did not alter synaptic transmission. Last, the inhibitory effect of oAβ42 peptide on synaptic transmission was prevented by 2-dimethylamino-4,5,6,7 tetrabromo-1H-benzimidazole (DMAT), a pharmacological inhibitor of CK2. Also, as predicted by DMAT experiments, microinjection of recombinant CK2 in the presynaptic terminal mimicked the oAβ42 effects on synaptic transmission, demonstrating that oAβ42 modulates synaptic transmission through a signaling pathway that requires CK2 activity at the presynaptic terminal. Our results show that acute injection of oAβ in the presynaptic compartment inhibits synaptic transmission on presynaptic stimulation, an effect that is molecularly associated with activation of synaptic CK2. These experiments allow us to envision a pharmacological intervention aimed at ameliorating the well-known early synaptic dysfunction widely described in AD.

Results

Acute Inhibition of Synaptic Transmission by Intracellular Oligomeric Aβ42 Peptides. To evaluate the effect of APP-derived peptides on synaptic transmission, presynaptic terminals were intracellularly microinjected with 10–100 nM of oAβ42 peptides or scrambled Aβ42 peptides under direct visualization by using fluorescent dye/peptide mix or FITC-labeled peptides (see *Materials and Methods*). Pre and postsynaptic potentials recorded simultaneously under current-clamp configuration were evoked by

NEUROSCIENCE
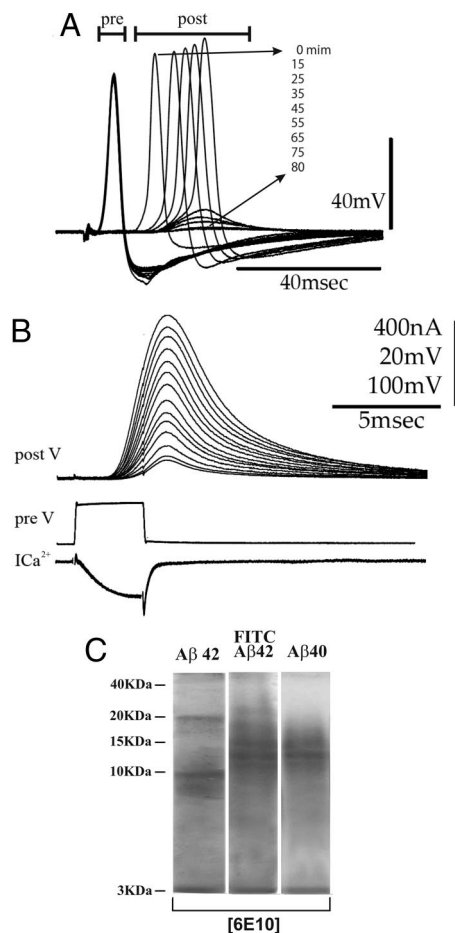
Fig. 1. Synaptic block after intraterminal injection oAβ42. (*A*) Pre- and postsynaptic spikes, after presynaptic microinjection of 100 nM oAβ42. The postsynaptic response was markedly reduced 80 min after oAβ42 injection. No significant change in presynaptic spike was observed. (*B*) Simultaneous recording of presynaptic calcium currents (ICa²⁺) and EPSP (post V) evoked by a depolarizing voltage-clamp step (pre V) after a single microinjection of 100 nM oAβ42 at the preterminal axon. Note that PSP decreased in amplitude, whereas presynaptic ICa^{2+} amplitude and time course were unaltered. (*C*) Identification of Aβ oligomers. Peptides were prepared as described in *Materials and Methods*, and assessed by Western blotting, using the primary antibody Aβ 1-16 [6 E10]. Aβ42, FITC-Aβ42, and Aβ40. Note that Aβ42 oligomerized mainly as dimers (≈8-kDa band).

terminal electrical stimulation (9). Synaptic transmission triggered once every 2 s for 3 min was markedly reduced in the injected terminals. In the experiment illustrated in Fig. 1*A*, a clear reduction of the rate of rise of excitatory postsynaptic potential (EPSP) was observed at ≈15 min after the injection. The EPSP became subthreshold for the generation of action potentials after 55 min, and continued to decrease in amplitude over the next 80 min. In all experiments, the latency for the oAβ42 block depended on the injection site. For injections at the actual site of transmitter release, the preterminal digit itself, the blocking time was as short as 10 to 15 min. When injected distal to the release site, the block correlated with the diffusion time into the preterminal ≈20 to 35 min. In fact, in all cases, the blocking effect was not seen until the fluorophore reached the level of the preterminal, indicating that the blocking effect of oAβ42 was limited to the site of transmitter release. No significant effect in EPSP kinetics was observed after presynaptic terminal microinjection of scrambled Aβ42 peptides (*n* = 5).

To define the mode of action more strictly, fluorophore/

oAβ42 mix (*n* = 4) and FITC-labeled oAβ42 (*n* = 3) were tested to determine possible changes in the amplitude or duration of the presynaptic action potential. No significant effects were observed in either the amplitude or duration of the presynaptic action potential in these experiments (Fig. 1*A*), nor in those where presynaptic terminals were microinjected with scrambled Aβ42 peptides (*n* = 5).

Presynaptic Calcium Currents (ICa²⁺) Were Unaffected by Aβ42 Peptides. After the initial finding that transmission was altered by oAβ42 peptides, the possibility that the synaptic block was associated with changes in presynaptic calcium currents ICa²⁺ was tested. The amplitudes and time course of the presynaptic calcium currents were directly determined by presynaptic voltage-clamp steps (*n* = 4) (9). ICa²⁺ were determined at different time intervals after presynaptic injection of oAβ42 100 nM. The results indicated that neither the time course nor the amplitudes of the presynaptic calcium currents were altered during the synaptic block (Fig. 1*B*).

The oAβ42 Peptides Alter Synaptic Vesicle Availability. To determine whether oAβ42-induced depression of transmission was secondary to a reduction of transmitter release (as would be expected if the docking or mobilization of vesicles were impaired) or by a defect in synaptic vesicle fusion, a high-frequency presynaptic stimulation paradigm (50–100 Hz) was implemented.

Transmission in the squid giant synapse is phasic in nature, i.e., it cannot maintain a high level of release for a protracted time (10). Thus, a high-frequency stimulation protocol will rapidly deplete the transmitter (as evidenced by decrease in postsynaptic amplitude during a stimulus train) without affecting the amplitude of the presynaptic action potential (post 1 in Fig. 2*A*) (11). The time course of this decay gives an estimate of transmitter availability, a reflection of a decrease in either synaptic vesicle mobilization or docking (11). After a resting period of 15 min after this depression, synapses recovered their release capability (11). In contrast, synapses injected with 100 nM oAβ42 (*n* = 6) did not recover, but rather were further depressed after the resting period (post 2 in Fig. 2*A*), without modification of the presynaptic spike. A similar effect was observed in synapses injected with concentrations as low as 10 nM oAβ42.

However, synapses microinjected with scrambled Aβ42 (*n* = 5), as with uninjected synapses (11), recovered to their baseline normally after the high-frequency stimulation protocol, after 15-min rest (post 2 in Fig. 2*B*). These data indicate that oAβ42 specifically alters the availability of synaptic vesicles (11).

Extracellular oAβ42 Peptides Do Not Affect Synaptic Transmission. Because it has been reported that subacute/chronic exposure of neurons to oAβ42 peptides produces synaptic dysfunction (12), we tested the acute effect of these peptides extracellularly. Superfusion with oAβ42 peptides ranging from 100 nM to 1 mM during ≥90 min using low (*n* = 4) and high frequency (*n* = 4) stimulation protocols demonstrated no significant changes in synaptic transmission. These experiments indicate that the intracellular localization of oAβ42 is required to inhibit synaptic transmission.

Intracellular Toxicity of a Different APP Proteolytic Product. We tested the effects on synaptic transmission of oAβ40 (Fig. 1*C*), the predominant Aβ isoform normally produced and released extracellularly (13). Preterminal injection of 100 nM oAβ40 peptides produced no significant changes in presynaptic potential or EPSP amplitude (*n* = 4). High-frequency stimulation of oAβ40 injected presynaptically demonstrated a normal pattern of transmitter depletion and recovery (*n* = 9) (Fig. 2*C*; note that synaptic recovery, as opposed to the continuous deterioration of synaptic release, is the significant variable in this set of experi-
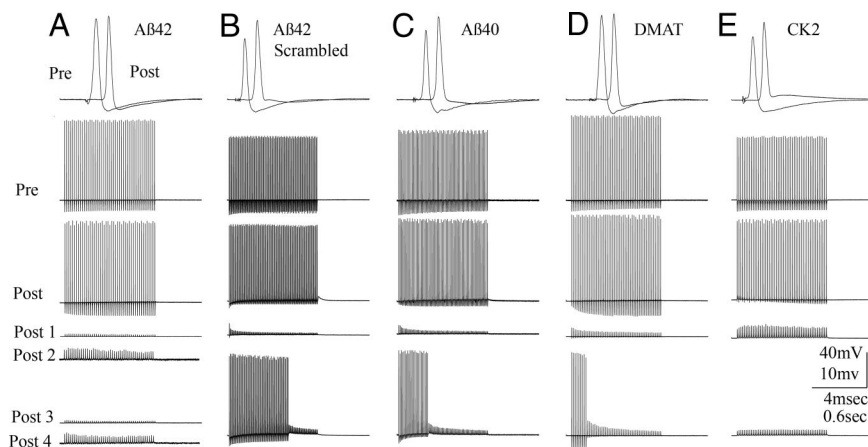
Fig. 2. Results from preterminal injection of oAβ42, oAβ40, Aβ42 scrambled, oAβ42 DMAT inhibitor, and CK2. Pre and postsynaptic responses were recorded (Pre/Post), and the presynaptic terminals were microinjected. The presynaptic axon was electrically stimulated (Pre) at 100 Hz, and the postsynaptic response recorded (Post). The trains were repeated once per second until failure of postsynaptic action potential generation was complete for all presynaptic pulses. After a 1-min rest, stimulus train sequences were repeated until the first train generated no postsynaptic spikes after the short rest. After a rest period of 15 min, a single stimulus train was given (post 2). At that point, the synapse would either show increased release failure (*A* and *E*) or recover (*B–D*). For further details, see *Results*.

ments). These findings indicate that it is mainly the Aβ42 fragment of the APP protein that mediates the synaptic dysfunction associated with AD.

CK2 Pathway Is Involved in oAβ42 Effect on Synaptic Transmission. The number of abnormal protein kinase activities in AD is extensive, including many serine/threonine kinases (GSK3, p38, JNK, cdk5, CK1, and CK2; see refs. 14, 15). To investigate the molecular mechanism by which oAβ42 inhibits synaptic transmission, we focused on the role of CK2, a kinase that regulates several intraaxonal regulatory processes related to synaptic transmission (16–18). Also, CK2 has been found in the extract of kinases that phosphorylate neurofilaments in the squid giant axon (19). Also, only oAβ42 inhibits fast axonal transport (FAT) in extruded squid axoplasms through a molecular mechanism that involves activation of CK2 activity. This activation leads to the inhibition of FAT of membrane-bounded organelles carried by the 2 most important FAT motors: dynein and kinesin-1.

Preterminal coinjection of oA42 (100 nM) with DMAT (5 μM), a potent and highly specific ATP-competitive inhibitor of CK2, produced almost complete reduction of the oAβ42 effect on the EPSP during the high-frequency stimulation protocol (post 2 in Fig. 2*D*) without affecting other aspects of synaptic transmission. Consistent with this finding, intrasynaptic microinjection of recombinant CK2 (4U) produced inhibition of synaptic transmission. In fact, the effect of CK2 on synaptic transmission was indistinguishable from that of oAβ42 peptides (post 2 in Fig. 2*E*). Thus, CK2 activity is required for the negative modulation of synaptic transmission produced at the squid synapse by the oAβ42 peptide.

Presynaptic Aβ42 Oligomers Produced Depletion of the Docked Synaptic Vesicle Pool After High-Frequency Presynaptic Stimulation, an Ultrastructural Correlate. Given our observation that intraterminal injection of oAβ42 peptide induced synaptic dysfunction without affecting presynaptic ionic currents, we expected that the oAβ42 peptide could induce changes at the presynaptic vesicle pools. In fact, given the large number of steps involved in synaptic vesicle availability, loading, or release, oAβ42 peptides could be expected to have specific inhibitory effects on transmitter release. To determine whether any of such steps was affected by the presynaptic oAβ injection, we implemented an ultrastructural analysis of the injected synapses. Stellate ganglia were rapidly

fixed (see *Materials and Methods*) after the electrophysiological (high-frequency stimulation protocol in oAβ42, scrambled Aβ42 or oAβ40 microinjected axons) experiments were concluded, 75–90 min after the injection. Fixed synapses were processed for ultrastructural microscopy (see *Materials and Methods*).

The ultrastructural results from 3 oAβ42-injected presynaptic terminals (Fig. 3) demonstrated a statistically significant ($P < 0.005$) decrease in the number of docked vesicles ($n = 20$ synaptic active zones) when compared with the number of vesicles from 38 active zones in the 4 control axons injected with scrambled Aβ42 (Fig. 3 and Table 1). Also, the oAβ42-injected terminals preserved the clathrin-coated vesicle (CCV) profiles, and produced a statistically significant increase in the number of nondocked vesicles in the vicinity of the active zone ($P < 0.027$). The images, as well as the quantitative analysis, indicate that oAβ42 injection results in the reduction of the docked synaptic vesicle pool at the presynaptic active zone, but does not prevent clathrin-dependent endocytosis (Fig. 3 and Table 1).

Discussion

Synaptic transmission dysfunction appears to be among the earliest events in the cognitive decline that characterizes AD, and has long been considered the best correlate of this decline (20). However, the cellular mechanisms involved in the synaptic transmission failure that is ultimately responsible for the cognitive decline have not been defined. Depressed synaptic transmission has been reported in AD mouse models of β amyloidosis, and is concomitant with the appearance of intraneuronal Aβ accumulation; it even precedes the formation of extracellular plaques (5). However, the nature of this accumulation and whether such plaques are toxic remain open questions. The experiments reported here indicate that preterminal oAβ42 peptides, but no other APP aggregated isoform (Aβ40), produced specific functional and structural abnormalities in an excitatory-chemical synapse. This finding provides a possible explanation of the molecular mechanisms underlying the early synaptic dysfunction in AD.

Toxicity of Intraneuronal Aβ: Does Length Matter? Extracellular accumulation of Aβ represents the foundation of the amyloid cascade hypothesis (21). In recent studies (21, 22), the level of intracellular Aβ accumulation has emerged as an important variable in the pathogenesis of AD. These studies, implemented
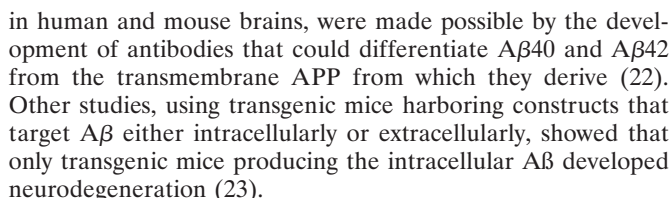
Fig. 3. Ultrastruture of scrambled oAβ42 (control) and oAβ42-injected presynaptic terminals. (*A* and *B*) Electron micrographs from cross sections of a scrambled oAβ42 injected synapse. (*A*) Low-magnification image showing 4 active zones with synaptic vesicle clusters (black dots); (*B*) higher magnification image of the same synapse showing 2 active zones (black dots) with many docked vesicles and a small set of CCVs at some distance from the active zone. (*C* and *D*) Electron micrographs from cross sections of an oAβ42-injected synapse. (*C*) Low-magnification image showing 2 active zones with only a few docked vesicles (black dots) and significantly large number of synaptic vesicle clusters some distance from the plasmmalema; (*D*) higher magnification image from the same synapse as in *C*, showing an active zone, with few docked vesicles and a large synaptic vesicle cluster in the vicinity.

Table 1. Quantitative EM analysis in the active zones of controls and oligomer Aβ₁₋₄₂-injected presynaptic terminals

	Normal	Clathrin-coated	Docked
Control	57.23 ± 4.75	4.62 ± 0.60	9.85 ± 0.71
Aβ1–42	75.12 ± 6.13*	3.65 ± 0.39	4.09 ± 0.46**

Vesicle number of synaptic vesicles per square micrometer, clustered at active zones (mean $\pm$ SD). *, $P < 0.027$. Docked vesicles are defined as those within 0.1 vesicle diameters of the plasma membrane at the active zone. **, $P < 0.005$. Clathrin-coated vesicles numbers are the mean number of CCV per square micrometer. Control, 100 nM scrambled Aβ42 injected synapses, $n = 20$ active zones; Aβ42 = 100 nM oAβ42 injected synapses, $n = 38$ active zones. Both types of synapses were fixed after the high-frequency stimulation protocol. Data are presented as the average of 4 synapses injected with scrambled Aβ42, and 3 injected with oAβ42.

secretory pathway (5). Other possible mechanisms that explain intracellular Aβ accumulation involve Aβ endocytosis (24). Thus, in organotypic hippocampal slice culture, Aβ42 gradually accumulates, and is retained intact by CA1 neurons, but not in other hippocampal subregions (25), suggestive of selective Aβ retention by neurons at risk in AD. Even more intriguing is the fact that oligomerization of Aβ associated with increased neurotoxicity has been identified within the neuronal cytosol (26).

Our experimental design allowed a direct investigation of the acute effects of extracellular and intracellular Aβ42 peptides on synaptic transmission. We demonstrated that oAβ42 results in a reduction of synaptic transmission only when injected intracellularly. However, our results do not completely rule out an extracellular effect, because it is known that glial cells take up Aβ peptides (27), and our preparation has abundant glial-like elements surrounding the synapse. However, more fundamentally, although the molecular basis for synaptic release has been known to be very similar in vertebrates and in squid (28), the transmembrane regulation of protein transport is not well defined in this invertebrate. Therefore, it is possible that extracellularly applied oAβ42 is incorporated into a different intracellular compartment or is only weakly incorporated. However, we do not favor these possibilities, because we saw no effects on synaptic transmission even when we increased the extracellular concentration of oAβ42 peptide by 5-fold.

Concerning the difference in toxicity between Aβ peptides, most of the full-length Aβ peptide produced is 40 residues in length (Aβ40), whereas ≈10% is the Aβ42 variant. Aβ40 is less hydrophobic and less prone to fibril formation than Aβ42 (29). Our data agree with such results in that concentrations of intraterminal oAβ40 comparable with those demonstrating synaptic block by oAβ42 peptides produced no significant changes in synaptic transmission. These data are also consistent with studies that used C-terminal-specific antibodies against Aβ40 and Aβ42, and found that most of the intracellular Aβ ends at residue 42 and not at 40 (5). Also, ImmunoGold ultrastructure has shown that Aβ42 can be found in neuronal multivesicular bodies in the human brain, where it is associated with synaptic pathology (30). Recent pathological findings using sequential brain extraction procedures demonstrated that the intracellular Aβ42 levels and membrane-bound compartments were significantly higher in the neocortex of AD cases than in controls, and were correlated with neurological deficit, whereas Aβ40 levels were similar in patients with AD and in controls (7).

Aβ-Related Axonal Pathology, Potential Targets, and Mechanism. Amyloidogenic mouse models have established that overproduction of Aβ leads to dystrophic axons and dendrites around amyloid plaques. It is also clear that anterograde axonal transport delivers Aβ peptide into plaques (31). Substantial controversy remains over the sites of APP processing and Aβ release.

in human and mouse brains, were made possible by the development of antibodies that could differentiate Aβ40 and Aβ42 from the transmembrane APP from which they derive (22). Other studies, using transgenic mice harboring constructs that target Aβ either intracellularly or extracellularly, showed that only transgenic mice producing the intracellular Aß developed neurodegeneration (23).

Some experimental evidence suggests that intracellular Aβ accumulates because a nonsecreted segment of the Aβ molecule remains in the cytosol. Given that the majority of Aβ is normally secreted, such results indicate that Aβ is predominantly cleaved at, or near, the plasmalemmal inner surface or as part of the

Some studies implicate the axon as a site of Aβ production (32). Consistent with this amyloid deposition hypothesis is the fact that plaque formation increases if poor axonal transport delays the progress of APP and its processing enzymes through the axon (8, 33). Other reports failed to reproduce parts of the model, in which APP and its processing enzymes are cotransported (34). Some Aβ release occurs at the synapse in an activity-dependent manner, but Aβ can be released from more proximal sites as well (31).

Also controversial is the issue of whether Aβ toxicity is an intracellular or an extracellular event. Intraaxonal accumulation of Aβ appears before extracellular Aβ when axons are damaged by deficiency of G protein-coupled receptor kinase-5 (GRK5) (35). However, extracellular Aβ42 causes axon abnormalities and death in primary culture (36). Our finding that intracellular oAβ42 triggers synaptic abnormalities, and the fact that Aβ42 is efficiently internalized (18), suggest that in subacute (≥90-min duration) mammalian experiments reporting neurotoxicity induced by extracellular oAβ42, the effect may in fact be mediated by internalization of the oAβ42.

From a pharmacological perspective, CK2 activity is a key element in synaptic modulation by oAβ42 peptides. Indeed, as shown in the accompanying article (39), CK2 activity induced by oAβ42 can reduce transmission by inhibiting FAT. However, CK2 has multiple substrates, and several of these are presynaptic proteins (37); consequently, oAβ42 may modify synaptic transmission through several targets and/or mechanisms. Our functional data rule out an effect on the properties of presynaptic calcium channels. The structural findings (depletion of the synaptic vesicle pool without affecting clathrin-dependent endocytosis) suggest the involvement of other molecular events such as the dynamin-dependent rapid synaptic vesicle endocytic pathway. Two pieces of information support this hypothesis: (*i*) disruption of dynamin/synaptophysin interaction at the squid presynaptic terminal causes functional and structural abnormalities of the synapse (11), similar to those reported here for intraaxonal oAβ42; and (*ii*) Aβ42 axonal internalization is dynamin-dependent.

In conclusion, this study indicates that intrasynaptic oAβ42, but not oAβ40, acutely inhibits transmission at the squid giant synapse. This inhibition is molecularly tied to a cascade of events involving CK2 activation and the rapid clathrin-independent endocytosis pathway. The reduction of FAT induced by oAβ42 showed in the accompanying article, in combination with our results showing a dramatic acute inhibition of synaptic transmission after intrasynaptic injection of oAβ42, represent novel findings concerning AD synaptic failure now clearly associated with a reduction of synaptic vesicle pools and transmitter release.

Materials and Methods

Electrophysiology and Microinjections. Stellate ganglia from the squid (*Loligo pealei*) were isolated from the mantle. The isolation of the ganglion and the electrophysiological techniques used have been described previously (9). Two electrodes were used in the presynaptic terminal, one for pressure microin-jection and voltage-clamp current feedback, and the second for monitoring membrane potential. The peptides were pressure-microinjected into the largest (most distal) presynaptic terminal digit, the total volume fluctuating between 0.1 and 1 pl (28). The exact location of injection and the diffusion and steady-state distribution of the peptide/fluorescent dye mix (0.001% dextran fluorescein) or the peptides labeled with FITC were monitored by using a fluorescence microscope attached to a Hamamatsu camera system. In all experiments, a correlation was made between the localization of the fluorescence and the electrophysiological findings.

Peptide Preparation. Aβ42, FITC, Aβ42, Aβ40, and scrambled Aβ42 peptides were obtained from American Peptide. Lyophilized Aβ peptides were resuspended in 1,1,1,3,3,3-hexafluoro-2-propanol (HFIP; Fluka); after drying, the pellets were diluted in DMSO (Sigma). Aβ/DMSO solutions were resuspended in PBS buffer to the desired concentration for 12 h before use, following Stine et al. (38). This peptide protocol induces oligomerization of Aβ peptides (see *Results* and Fig. 1*C*).

Electron Microscopy. The ganglia were removed from the electrophysiology recording chamber, fixed by immersion in glutaraldehyde, postfixed in osmium tetroxide, stained in block with uranium acetate, dehydrated, and embedded in resin (Embed 812, EM Sciences). Ultrathin sections were collected on pyoloform (Ted Pella), and carbon-coated single-slot grids and contrasted with uranyl acetate and lead citrate.

Morphometry and quantitative analysis of the synaptic vesicles were performed with a Zidas digitizing system (Zeiss) interfaced with a Macintosh G3 computer. Electron micrographs were taken at an initial magnification of 16,000 and 31,500×, and photographically enlarged to a magnification of 40,000 and 79,000× for counting synaptic vesicles and CCV, respectively. Vesicle density at the synaptic active zones was determined as the number of vesicles per square micrometer, on an average area of 0.8 μm^2 per active zone. CCV density was determined within the limits of the presynaptic terminal on an average terminal area of 3.3 μm^2. Three different oAβ42-injected terminals and 4 control terminals (scrambled Aβ42, all of which demonstrated no release defects) were examined. The number of docked and undocked vesicles was determined from a total of 20 active zones for the oAβ42 and 36 active zones for the scrambled Aβ42 controls (Table 1).

Pharmacological Tools. DMAT (Calbiochem), recombinant-active CK2 (New England Biolabs).

Western Blottings. Samples were subjected to 18% PAGE-SDS, using 10 ng per lane of the peptides (Aβ42, FITC Aβ42, and Aβ40). The SDS/PAGE was loaded and transferred to nitrocellulose, UV cross-linked, and blocked for 1 h in 1% BSA, 1% hemoglobin in TBSN (10 mM Tris·HCl/150 mM NaCl/0.2% Nonidet P-40). The nitrocellulose was incubated for 24 h in primary antibody Aβ 1-16 [6 E10] (1:500; Covance), washed 3 times with TBSN, and then incubated for 1 h in secondary antibody (antimouse-conjugated to alkaline phosphatase) (1:1,000; Sigma). Blots were developed with 5-bromo-4-chloro-3-indolyl phosphate/nitro blue tetrazolium (Promega).

1. Hutton M, Pérez-Tur J, Hardy J (1998) Genetics of Alzheimer's disease. *Essays Biochem* 33:117–131. Review.
2. Younkin SG (1998) The role of A beta 42 in Alzheimer's disease. *J Physiol Paris* 92:289–292.
3. Sisodia SS, Kim SH, Thinakaran G (1999) Function and dysfunction of the presenilins. *Am J Hum Genet* 65:7–12.
4. Selkoe DJ (2001) Alzheimer's disease: Genes, proteins, and therapy. *Physiol Rev* 81:741–766.
5. LaFerla FM, Green KN, Oddo S (2007) Intracellular amyloid-beta in Alzheimer's disease. *Nat Rev Neurosci* 8:499–509.
6. Giannakopoulos P, et al. (2003) Tangle and neuron numbers, but not amyloid load, predict cognitive status in Alzheimer's disease. *Neurology* 60:1495–1500.
7. Steinerman JR, et al. (2008) Distinct pools of beta-amyloid in Alzheimer disease-affected brain: A clinicopathologic study. *Arch Neurol* 65:906–912.
8. Lee EB, et al. (2005) BACE overexpression alters the subcellular processing of APP and inhibits Abeta deposition in vivo. *J Cell Biol* 168:291–302.
9. Llinás R, Steinberg IZ, Walton K (1981) Relationship between presynaptic calcium current and postsynaptic potential in squid giant synapse. *Biophys J* 33:323–351.
10. Kusano K, Landau EM (1975) Depression and recovery of transmission at the squid giant synapse. *J Physiol* 245:13–32
11. Daly C, Sugimori M, Moreira JE, Ziff EB, Llinás R (2000) Synaptophysin regulates clathrin-independent endocytosis of synaptic vesicles. *Proc Natl Acad Sci USA* 97:6120–6125.
12. Puzzo D, et al. (2005) Amyloid-beta peptide inhibits activation of the nitric oxide/cGMP/cAMP-responsive element-binding protein pathway during hippocampal synaptic plasticity. *J Neurosci* 25:6887–6897.
13. Chang KA, Suh YH (2005) Pathophysiological roles of amyloidogenic carboxy-terminal fragments of the beta-amyloid precursor protein in Alzheimer's disease. *J Pharmacol Sci* 97:461–471.
14. Petersen RB, et al. (2007) Signal transduction cascades associated with oxidative stress in Alzheimer's disease. *J Alzheimers Dis* 11:143–152.
15. Milton NG (2005) Phosphorylated amyloid-beta: The toxic intermediate in alzheimer's disease neurodegeneration. *Subcell Biochem* 38:381–402.
16. Raftery M, et al. (2005) Phosphorylation of apolipoprotein-E at an atypical protein kinase CK2 PSD/E site in vitro. *Biochemistry* 44:7346–7353.

17. Hilfiker S, Pieribone VA, Nordstedt C, Greengard P, Czernik AJ (1999) Regulation of synaptotagmin I phosphorylation by multiple protein kinases. *J Neurochem* 73:921–932.
18. Lieberman DN, Mody I (1999) Casein kinase-II regulates NMDA channel function in hippocampal neurons. *Nat Neurosci* 2:125–132.
19. Takahashi M, Amin N, Grant P, Pant HC (1995) P13suc1 associates with a cdc2-like kinase in a multimeric cytoskeletal complex in squid axoplasm. *J Neurosci* 15:6222–6229.
20. Coleman PD, Yao PJ (2003) Synaptic slaughter in Alzheimer's disease. *Neurobiol Aging* 24:1023–1027.
21. Hardy JA, Higgins GA (1992) Alzheimer's disease: The amyloid cascade hypothesis. *Science* 256:184–185.
22. Gouras GK, Almeida CG, Takahashi RH (2005) Intraneuronal Abeta accumulation and origin of plaques in Alzheimer's disease. *Neurobiol Aging* 26:1235–1244.
23. LaFerla FM, Tinkle BT, Bieberich CJ, Haudenschild CC, Jay G (1995) The Alzheimer's A beta peptide induces neurodegeneration and apoptotic cell death in transgenic mice. *Nat Genet* 9:21–30.
24. D'Andrea MR, Nagele RG, Wang HY, Peterson PA, Lee DH (2001) Evidence that neurones accumulating amyloid can undergo lysis to form amyloid plaques in Alzheimer's disease. *Histopathology* 38:120–134.
25. Bahr BA, et al. (1998) Amyloid beta protein is internalized selectively by hippocampal field CA1 and causes neurons to accumulate amyloidogenic carboxyterminal fragments of the amyloid precursor protein. *J Comp Neurol* 397:139–147.
26. Takahashi RH, et al. (2004) Oligomerization of Alzheimer's beta-amyloid within processes and synapses of cultured neurons and brain. *J Neurosci* 24:3592–3599.
27. LeBlanc AC, Xue R, Gambetti P (1996) Amyloid precursor protein metabolism in primary cell cultures of neurons, astrocytes, and microglia. *J Neurochem* 6:2300–2310.
28. Llinas R (1999) *The Squid Giant Synapse: A Model for Chemical Transmission* (Oxford Univ Press, New York).
29. Li QX, et al. (1999) Intracellular accumulation of detergent-soluble amyloidogenic A beta fragment of Alzheimer's disease precursor protein in the hippocampus of aged transgenic mice. *J Neurochem* 72:2479–2487.
30. Almeida CG, Takahashi RH, Gouras GK (2006) Beta-amyloid accumulation impairs multivesicular body sorting by inhibiting the ubiquitin-proteasome system. *J Neurosci* 26:4277–4288.
31. Adalbert R, Gilley J, Coleman MP (2007) Abeta, tau and ApoE4 in Alzheimer's disease: The axonal connection. *Trends Mol Med* 13:135–142.
32. Muresan Z, Muresan V (2006) Neuritic deposits of amyloid-beta peptide in a subpopulation of central nervous system-derived neuronal cells. *Mol Cell Biol* 26:4982–4997.
33. Stokin GB, et al. (2005) Axonopathy and transport deficits early in the pathogenesis of Alzheimer's disease. *Science* 307:1282–1288.
34. Lazarov O, et al. (2005) Axonal transport, amyloid precursor protein, kinesin-1, and the processing apparatus: Revisited. *J Neurosci* 25:2386–2395.
35. Li L, Liu J, Suo WZ (2008) GRK5 deficiency exaggerates inflammatory changes in TgAPPsw mice. *J Neuroinflammation* 5:24.
36. Song MS, Saavedra L, de Chaves EI (2006) Apoptosis is secondary to non-apoptotic axonal degeneration in neurons exposed to Abeta in distal axons. *Neurobiol Aging* 27:1224–1238.
37. Blanquet PR (2000) Casein kinase 2 as a potentially important enzyme in the nervous system. *Prog Neurobiol* 60:211–246.
38. Stine WB, Jr, Dahlgren KN, Krafft GA, LaDu MJ (2003) In vitro characterization of conditions for amyloid-beta peptide oligomerization and fibrillogenesis. *J Biol Chem* 278:11612–11622.
39. Pigino G, et al. (2009) Disruption of fast axonal transport is a pathogenic mechanism for intraneuronal amyloid beta. *Proc Natl Acad Sci USA*, in press.